JPP Journal of Pharmacy and Pharmacology

JPP 2005, 57: 1475–1484

Received February 14, 2005
Accepted June 22, 2005
DOI 10.1211/jpp.57.11.0014
ISSN 0022-3573

Statin-induced apoptosis linked with membrane farnesylated Ras small G protein depletion, rather than geranylated Rho protein

Sumio Matzno, Shinya Yasuda, Sachiko Juman, Yukiko Yamamoto, Noriko Nagareya-Ishida, Keiko Tazuya-Murayama, Toshikatsu Nakabayashi and Kenji Matsuyama

Abstract

Rhabdomyolysis is a severe adverse effect of 3-hydroxy-3-methylglutaryl-coenzyme A reductase inhibitors (statins). This myopathy is strongly enhanced by the combination with statins and fibrates, another hypolipidaemic agent. We have evaluated the initial step of statin-induced apoptosis by the detection of membrane flip-flop using flow cytometric analysis. L6 rat myoblasts were treated with various statins (atorvastatin (3 μM), cerivastatin (3 μM), fluvastatin (3 μM), pravastatin (3 mM), or simvastatin (3 μM)) for 2, 4 or 6 h followed by reacting with FITC-conjugated annexin V for the detection of initial apoptosis signal (flip-flop). Various statin-treated myoblasts were significantly stained with FITC-annexin V at 6 h, whereas they were not detected at 2 h. Moreover, immunoblot analysis indicated that when the cells were treated with cerivastatin (3 μM), membrane-associated Ras protein was activated and detached until 6 h, resulting in cell death through the consequent activation of caspase-8. On the other hand, since cytosolic Ras activation did not activate, there is still an unknown mechanism in statin-related Ras depletion. In conclusion, statin-induced apoptosis in muscular tissue was directly initiated by the farnesyl-anchored Ras protein depletion from cell membrane with subsequent apoptosis.

School of Pharmaceutical Sciences, Mukogawa Women's University, 11-68, Kyuban-cho, Koshien, Nishinomiya, Hyogo 663-8179, Japan

Sumio Matzno, Shinya Yasuda, Sachiko Juman, Yukiko Yamamoto, Noriko Nagareya-Ishida, Toshikatsu Nakabayashi, Kenji Matsuyama

Daiichi University, College of Pharmaceutical Sciences, 22-1, Tamagawa-cho, Minami-ku, Fukuoka 815-8511, Japan

Keiko Tazuya-Murayama

Correspondence: S. Matzno, First Department of Biochemistry, School of Pharmaceutical Sciences, Mukogawa Women's University, 11-68, Kyuban-cho, Koshien, Nishinomiya, Hyogo 663-8179, Japan. E-mail: smatzno@mwu.mukogawa-u.ac.jp

Acknowledgements: The authors are grateful to Miss Yayoi Kamakura for her technical support with the flow cytometry. We also thank Miss Naoko Inamuro and Miss Yukie Ogi for the immunoblotting study.

Introduction

Hyperlipidaemia is a major risk factor for cardio- and cerebrovascular disease and a number of hypolipidaemic agents are in clinical use for the control of plasma lipid levels that cause these diseases (Hess et al 2000; Rubins 2000). 3-Hydroxy-3-methylglutaryl-coenzyme A (HMG-CoA) reductase (EC 1.1.1.34) is the major rate-limiting enzyme in the pathway of cholesterol biosynthesis at the level of mevalonate production (Rodwell et al 1976). Therefore, inhibitors of this enzyme (statins) are widely used for patients with hypercholesterolaemia. However, there are adverse effects associated with statin administration. One of the most severe is rhabdomyolysis, which has the clinical signs of diffuse myalgia, muscle tenderness and elevation of blood creatinine phosphokinase concentrations (Vu et al 2001). A greater incidence of myopathy is caused by the administration of statins in combination with ciclosporin (Smith et al 1991) or fibric acids (Shek & Ferrill 2001). Several clinical studies alerted to the massive rhabdomyolysis and life threatening hyperkalaemia in a patient administered the combination of cerivastatin and gemfibrozil (Rubins 2000; Hendriks et al 2001; Shek & Ferrill 2001; Marsa-Carretero et al 2002). Recent in-vitro (Matzno et al 2003) and in-vivo (Matsuyama et al 2002) studies demonstrated exactly the clinical myopathy following coadministration of statins and fibrates. Additional in-vitro evaluation suggested that this myopathy caused skeletal apoptosis. Several previous reports suggested the depletion of a certain isoprenoid intermediate, which anchored Rho and Ras small G proteins to the cell membrane, inhibited cell proliferation in vascular smooth muscle (Blanco-Colio et al 2002), mesangial cells (Danesh et al

2002) and endothelial cells (Danesh et al 2003). However, the onset mechanism of myopathy is still controversial. Moreover, statin-induced cytotoxicity has only occurred in skeletal tissue in-vivo, suggesting that a specific pathway for statin-related apoptosis induction might exist in skeletal tissue. Therefore, in this study, we have aimed at clarification of statin-induced apoptosis directly using a skeletal myoblast cell line.

We have demonstrated the relationship between apoptotic initiation and membrane isoprenoid proteins (such as Ras, Rho and Cdc42). To detect an early step of apoptosis, we used fluorescent-conjugated annexin V that bound translocated phosphatidylserine from the inner face of the plasma membrane to the cell surface after initiating apoptosis (Zhang et al 1997). We examined caspase activity to speculate the statin-associated apoptosis pathway(s).

Materials and Methods

Materials

Atorvastatin, cerivastatin, fluvastatin, pravastatin and simvastatin were kindly gifted from Sankyo Pharmaceutical Corporation (Tokyo, Japan). Transferrin was purchased from Gibco (Carlsbad, CA), BSA, FITC-conjugated annexin V (FITC-annexin V), propidium iodide and insulin were from Sigma (St Louis, MA, USA). Collagenase was bought from Wako Pure Chemicals (Osaka, Japan). Specific substrates, acetyl-Asp-Glu-Val-Asp-7-amino-4-trifluoromethylcoumarin (Ac-DEVD-AFC) for caspase-3, Ac-Ile-Glu-Thr-Asp-7-amino-4-methylcoumarin (Ac-IETD-AMC) for caspase-8 and Ac-Leu-Glu-His-Asp-AFC (Ac-LEHD-AFC) for caspase-9 were bought from Biomol Research Laboratories, Inc. (Plymouth Meeting, PA, USA). All other materials were from Nacalei Tesque Ltd (Kyoto, Japan). Drugs were dissolved in dimethylsulfoxide (DMSO) and stored at 4°C until use. For the experiments, the control vehicle or drug solutions were added into the medium. The final concentration of DMSO did not exceed 0.3% (V/V).

Cell culture

L6 rat skeletal myoblasts were subcloned (designated G3H6) and were referred to simply as L6 (Matzno et al 1997, 2003). They were routinely maintained in the growth medium (alpha-minimum essential medium (α-MEM) containing 50 IU mL^{-1} benzylpenicillin (penicillin G), 50 μg mL^{-1} streptomycin and 10% FBS), and less than 20 passages were used in the experiments.

Generally, myoblasts (3×10^4 cells cm^{-2}) were seeded into tissue culture plates for subsequent experiments. Twenty-four hours after cultivation with growth medium, the medium was changed to differentiation medium (α-MEM supplemented with 1 mg mL^{-1} BSA, 10 μg mL^{-1} insulin, 5 μg mL^{-1} transferrin and 10 nM sodium selenite) to generate myotube formation, and incubated with statins for a further 2, 4 or 6 h. Statin-treated cells were provided for subsequent apoptotic analyses.

Microscopic observation

Cells were grown and differentiated on cover slips as described by Matzno et al (2003). Two, four or six hours after drug treatment in differentiation medium, the glass was removed and washed twice with phosphate-buffered saline (PBS). The cells were incubated with 10 μL reaction buffer (140 mM NaCl, 2.5 mM $CaCl_2$, 10 mM HEPES, pH 7.5) containing 12 μg mL^{-1} FITC-annexin V and 10 μg mL^{-1} propidium iodide for 10 min under dark conditions. After washing twice with PBS, the apoptotic myoblasts were observed with a fluorescein microscope under blue wavelength excitation.

Flow cytometric analysis

For the flow cytometric study, cells were seeded onto a microporous membrane of cell culture-insert (Transwell, Corning Coaster Corporation, Cambridge, MA, USA). At 0, 2, 4 or 6 h after drug application, membrane-associated cells were treated with collagenase solution (0.1% collagenase in α-MEM with 1% FBS) for 5 min at 37 °C and suspended. After washing twice with PBS, cells were incubated with FITC-annexin V and propidium iodide as mentioned above. Flow cytometric profiles were determined with FACSCalibur analyser and CELLQuest software (Becton Dickinson Immunocytometry Systems, Mountain View, CA, USA) at an excitation of 488 nm argon laser.

Membrane and cytosolic G proteins

Cells were seeded onto 100-mm tissue culture dishes (Asahi Techno Glass, Chiba, Japan) and cultured for 24 h with growth medium. The growth medium was then replaced with differentiation medium, and cerivastatin (3 μM) was added. The cells were incubated for a further 2, 4 or 6 h. The cells were harvested in PBS (containing 1 mM EDTA, 5 μM phenylmethyl sulfonyl fluoxide, 0.5 mM sodium molybdate and 2 μg mL^{-1} leupeptin) using a rubber policeman, sonicated for a few seconds followed by supercentrifugation at 50 000 g for 30 min at 4°C. Membrane (precipitate) and cytosolic (supernatant) fractions were collected and their protein contents were determined using the bicinchoninate protein assay (Pierce, Rockfold, IL, USA) with BSA as a standard. SDS-polyacrylamide gels used to separate phosphorylated from non-phosphorylated proteins contained an acrylamide/bisacrylamide ratio of 30:0.3 (Towatari et al 1995; Kitta et al 2001). Electrophoresis was performed onto 12.5% T gel and the separated proteins were electrotransferred to membrane at 180 mA for 1 h. After washing membrane twice with Tris-buffered saline containing 0.1% Tween 20

(TBST; 0.1% Tween 20, 150 mM NaCl and 10 mM Tris-HCl, pH 7.4), the blots were blocked in 5% skim milk for 1 h. The primary antibodies against Ras and Rho proteins (Lab Vision Corp., Fremont, CA, USA, 1:500 dilution with TBST containing 0.1% BSA) were applied for 1 h. After washing four times with TBST, membrane was treated with peroxidase-conjugated anti-mouse IgG (Amersham Pharmacia Biotech, Arlington Heights, IL, USA, 1:5000 dilution) for 1 h followed by enhanced chemiluminescence detection of antigens (Amersham). To determine the activated Ras content, Ras-GTP protein was precipitated using Raf-1 Ras binding domain conjugated agarose beads (Upstate Group Inc., Lake Placid, NY, USA). After washing with Mg^{2+}-containing lysis buffer (25 mM HEPES, 1% NP-40, 150 mM NaCl, 10 mM $MgCl_2$, 25 mM NaF, 1 mM EDTA, 1 mM Na_2VO_4 and 10 $\mu g\,mL^{-1}$ leupeptin, pH 7.4), precipitated proteins were assessed for Western blotting analysis.

Determination of caspase activity

Caspase activity was assessed by the cleavage of their specific substrates (Thornberry et al 1997). Briefly, 24 h after drug treatment, cells were washed twice with PBS and scraped. They were harvested with 0.1% Triton X-100 and centrifuged at 4000 g for 10 min at 4°C. Three samples of supernatant were incubated at 37°C with an equal volume of reaction buffer (100 mM NaCl, 50 mM HEPES, 1 mM EDTA and 10% glycerol, pH was adjusted at 7.4 by NaOH) and 50 μM of caspase specific substrates as described above (Ac-DEVD-AFC for caspase-3, Ac-IETD-AMC for caspase-8 and Ac-LEHD-AFC for caspase-9). After the 2-h reaction, production of 7-amino-4-trifluoromethylcoumarin (AFC) and 7-amino-4-methylcoumarin (AMC) were detected in a CytoFluor Plate Reader (PerSeptive Biosystems, Foster City, CA, USA) using an excitation wavelength of 360 nm/emission 530 nm and excitation 360 nm/emission 460 nm, respectively.

Statistical analysis

The data were expressed as mean ± s.d. Statistical significance was assessed using analysis of variance with randomized block (Figure 4) or one-way (Figure 6) design, and then compared using the Dunnett's method. A P value of 0.05 or less was considered as statistically significant.

Results

Early stage apoptosis in statin-treated myoblasts

Figure 1A shows the typical patterns of early apoptotic cells after cerivastatin treatment. The initial step of apoptosis was detected with FITC-annexin V, which specifically binds to membrane phosphatidylserine. Obviously, membrane phospholipids have asymmetrical distribution; most phosphatidylserine is located in the inner half of the lipid bilayer. However, when the apoptotic signal comes, phosphatidylserine translocates to the cell surface, thus, this stage results in the cells being stained with green fluorescence by FITC-annexin V. The cells then begin to die and so red fluorescence derived from propidium iodide was observed.

Time course of apoptosis initiation

Figure 1B shows the typical microscopic observation of simvastatin-induced apoptosis in L6 myoblasts. FITC-stained myoblasts were not observed at 2 h after statin treatment, they were first detected at 4 h and green-stained cells were time-dependently generated. Finally, dead cells were stained with propidium iodide because of the absence of dye-exclusion ability, that is, cell death as a result of apoptosis was detected as dual fluorescence of FITC and propidium iodide. Indeed, dual-fluorescent myoblasts had increased at 6 h. Figure 2 shows various statin-treated myoblasts at 6 h. A number of green fluorescent myoblasts were grown in cells treated with 3 μM cerivastatin (Figure 2C) and simvastatin (Figure 2F). The other statin-treated cells did not show a clear increase.

Flow cytometry

To determine the apoptotic cell rate a quantitative analysis was performed using an immunofluorescence flow cytometry assay. Figure 3 shows a typical flow cytometry pattern of simvastatin-treated myoblasts. Forward and side light scatter showed two peaks of population (data not shown), therefore we selected a myoblast-derived population. Red (propidium iodide, PI) and green (FITC) fluorescence histograms revealed that simvastatin-treated myoblasts caused an obvious population to emerge, which was stained with FITC-annexin V and propidium iodide (circled) at 4 (B) to 6 h (C). The agents affected cellular apoptosis time-dependently.

The appearance of apoptosis after various statin treatments is shown in Figure 4. Cerivastatin (3 μM) and simvastatin (3 μM) significantly increased green- and red-fluorescent (i.e. apoptosis) cell populations (circle) with the 6-h treatment. Pravastatin (3 mM) also increased apoptotic cells, however the concentration needed was a thousandfold that of cerivastatin and simvastatin. The other statins (3 μM) caused only slight or no increments of the apoptotic populations at 6 h.

Membrane-anchored small G proteins

The isoprenoid depletion might inhibit cellular proliferation in various tissues via membrane-anchored Rho and/or Ras, therefore, we measured membrane-associated and cytosolic small G protein contents using immunoblot analysis by enhanced chemiluminescence detection. To separate phosphorylated (GTP-bound) from unphosphorylated (GDP-bound) proteins,

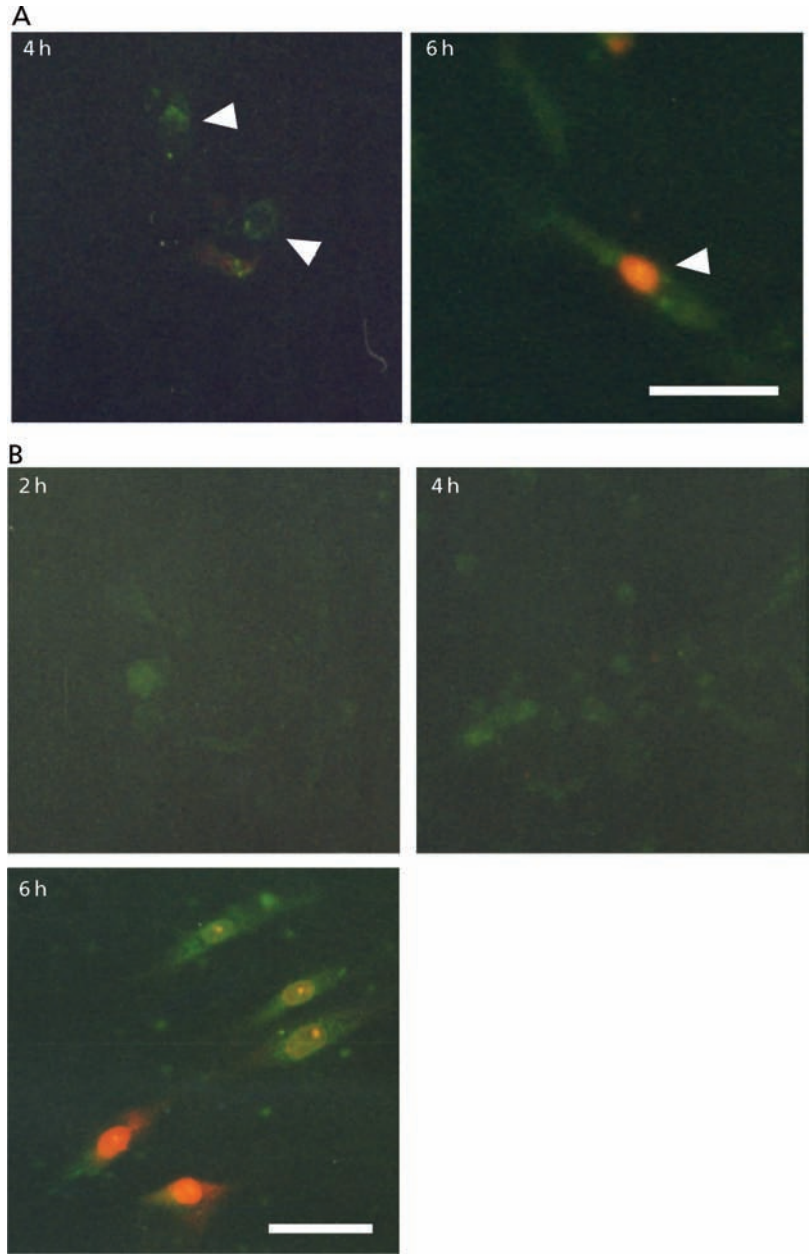

Figure 1 Fluorescent microscopic observation of statin-induced apoptosis. Typical fluorescent staining patterns of early (4 h) and late (6 h) apoptotic cells were found in cerivastatin-treated cells (A). Early stage apoptosis was shown in green fluorescence and late stage was shown as dual-stained. Each typical cell is indicated by an arrow. In B, L6 was treated with 3 μM simvastatin for 2, 4 or 6 h in differentiation medium and stained with FITC-annexin V and propidium iodide. Bar: 50 μm.

the ratio of bisacrylamide was reduced from the standard Laemmli-type gel (Towatari et al 1995; Kitta et al 2001). As shown in Figure 5A, activated Ras protein that bound to GTP showed upward shift and two populations (GTP-form and GDP-form) were apparently determined. The treatment of myoblasts with cerivastatin (3 μM) time-dependently decreased membrane active Ras, and it had disappeared completely at 6 h. Interestingly, membrane Ras depletion only occurred in activated protein, whereas 'inactivated' Ras did not diminish from the membrane. The same phosphorylated Ras depletion was observed in pravastatin-treated myoblasts, however, the 'activated' G protein content was lower than that of cerivastatin-treated myoblasts.

We evaluated the effect of statins on Ras activation using active-Ras specific precipitation methods. Activated Ras was precipitated with Raf-1 RBD agarose that specifically bound to activated Ras. As shown in Figure 5B, Raf-1 precipitated Ras was only found in the membrane fraction of samples. However, the amount of membrane-associated active Ras was markedly increased in cerivastatin-treated myoblasts. These data suggested that cerivas-

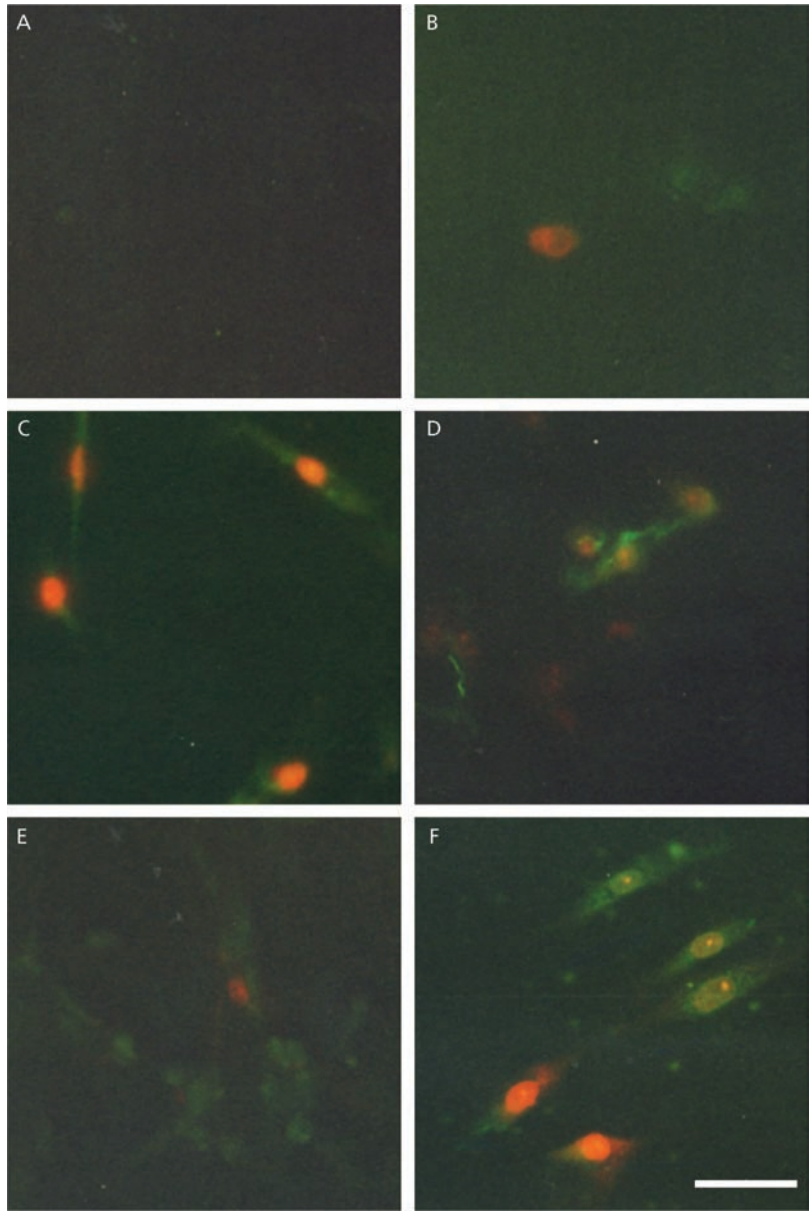

Figure 2 Effects of various statins on the onset of skeletal apoptosis in-vitro. L6 was incubated with various statins for 6 h. A, control; B, atorvastatin (3 μM); C, cerivastatin (3 μM); D, fluvastatin (3 μM); E, pravastatin (3 mM); and F, simvastatin (3 μM). Bar: 50 μm.

tatin itself activated Ras protein and subsequently activated Ras selectively fell into cytosol.

In contrast, there were no significant changes in membrane and cytosolic contents of Rho, another membrane-anchored G protein family (Figure 5C). This suggested that membrane Rho behaviour did not associate with statin-induced myopathy.

Caspase activity

Intracellular caspase activity was determined using selective substrates (see Materials and Methods). Twenty-four hours after drug treatment, cerivastatin (3 μM) and pravastatin (3 mM) significantly elevated caspase-3 (Figure 6A) and caspase-8 (Figure 6B) activity in differentiating L6 myoblasts. In contrast, they did not activate caspase-9 (Figure 6C) or caspase-12 (data not shown). These protease activities indicated that statins initially depressed the farnesyl isoprenoid contents by their production reducing, subsequently membrane Ras was diminished at 6 h, and consequently executed the apoptosis programme through a caspase-8-mediated pathway.

Discussion

It deserves special mention that there was a few hours delay through onset of apoptosis: generally, death

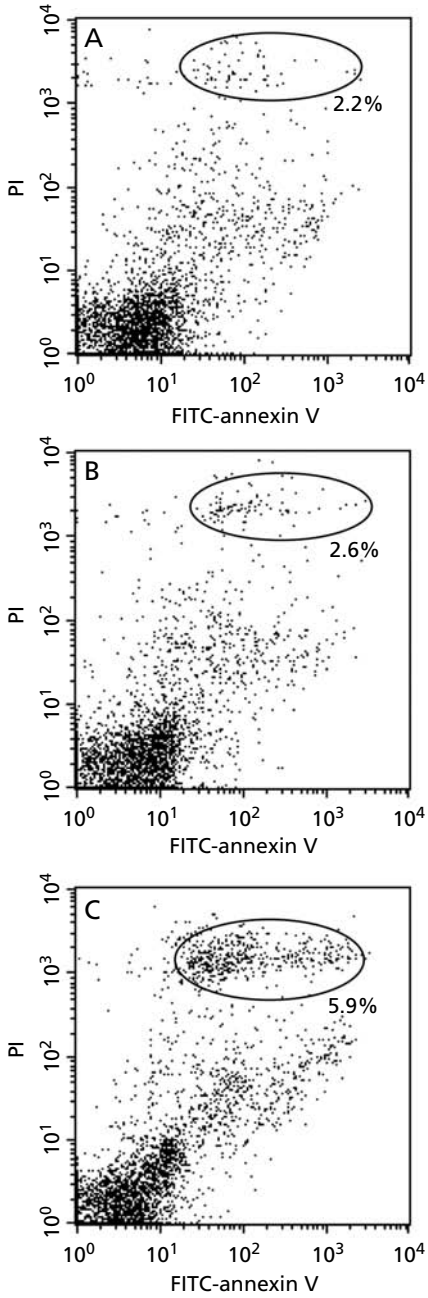

Figure 3 Time-dependent apoptosis generation in simvastatin-treated L6 myoblasts. L6 was incubated with 3 μM simvastatin for 2 (A), 4 (B) or 6 h (C), treated with FITC-annexin V and propidium iodide (PI) and assessed for flow cytometry. A circle indicates dual-staining population, which was evaluated as apoptotic cell particles.

ligand-mediated apoptosis occurs within 2 h. In contrast, annexin V-positive cells were initially detected at 4 h in statin-treated myoblasts (Figures 2 and 5). This demonstrated that statin application into myoblasts caused apoptosis through a certain initiation pathway. Therefore, we focused on HMG-CoA-reductase-mediated enzymology.

The cholesterol synthesis pathway is shown in Figure 7. HMG-CoA reductase mediates upstream of this pathway, and so several important intermediates are also reduced, such as farnesyl pyrophosphate and geranylgeranyl pyrophosphate (Takemoto & Liao 2001). Ras and Rho small G proteins play crucial roles in cell growth and differentiation. For the activation and signal transduction to downstream, they must be anchored to the plasma membrane through farnesyl and geranyl residues that covalently bind to the C-terminal of Ras and Rho proteins, respectively. However, our current immunoblotting analyses (Figures 6 and 7) showed that statins caused reduction in membrane Ras protein only, the membrane bound Rho protein level did not change in drug-treated L6 myoblasts. This suggested that statin-induced cytotoxicity was related to membrane Ras depletion.

Indeed, several investigators have reported the changes of membrane isoprenoid proteins in statin-treated cells. Ohnaka et al (2001) showed statin-related Rho-kinase inhibition in osteoclasts. Rho-related cell proliferation was inhibited by statins in smooth muscle and mesangial cells (Blanco-Colio et al 2002; Danesh et al 2002). This cytotoxicity was reduced by addition of geranyl pyrophosphate, not farnesyl pyrophosphate (Guijarro et al 1998), suggesting that statin-related cytotoxicity clearly associated with membrane Rho depletion in vascular tissues. It is also considered that Rho signal depletion by statin application is coupled with prevention of cardiac hypertrophy (Laufs et al 2002). A more recent study has indicated that Rho-dependent signal transduction is therefore considered as the main target of side effects in many tissues (Blanco-Colio et al 2003).

Our study revealed that selective depression of membrane Ras protein was found in apoptotic skeletal muscles (Figure 5A, B) in-vitro, whereas there was no depression of membrane Rho protein (Figure 5C). This was probably because severe apoptosis of skeletal tissue was caused via a disconnection of Ras-related signal(s), whereas the reduction in isoprenoid improved coronary heart disease was via the Rho-dependent pathway. Moreover, Ras depletion from the cell membrane specifically occurred in the GTP-bound form (Figure 5B), suggesting that the Ras-dependent signal was quickly and completely blocked by statins, and consequently skeletal myocytes were led to death.

More recently, three major cascades have been advocated for cellular apoptosis. Firstly, the certain 'death ligand' mediated pathway like Fas ligand and tumour necrosis factor (TNF) acts through caspase-8 and subsequent caspase-3 activation (Zimmermann et al 2001). Secondly, the mitochondria-mediated pathway acts through caspase-dependent and/or independent mechanisms (Ravagnan et al 2002). Thirdly, the endoplasmic reticulum mediated apoptosis was partially associated with intracellular calcium release and, in part, with activation of caspase-12 (Morishima et al 2002). Since this investigation suggested that statins directly affected Ras-related signal transduction (Figure 5), it was conceivable that these drugs would activate the ligand-mediated pathway through membrane Ras detachments. Furthermore, Kazama &

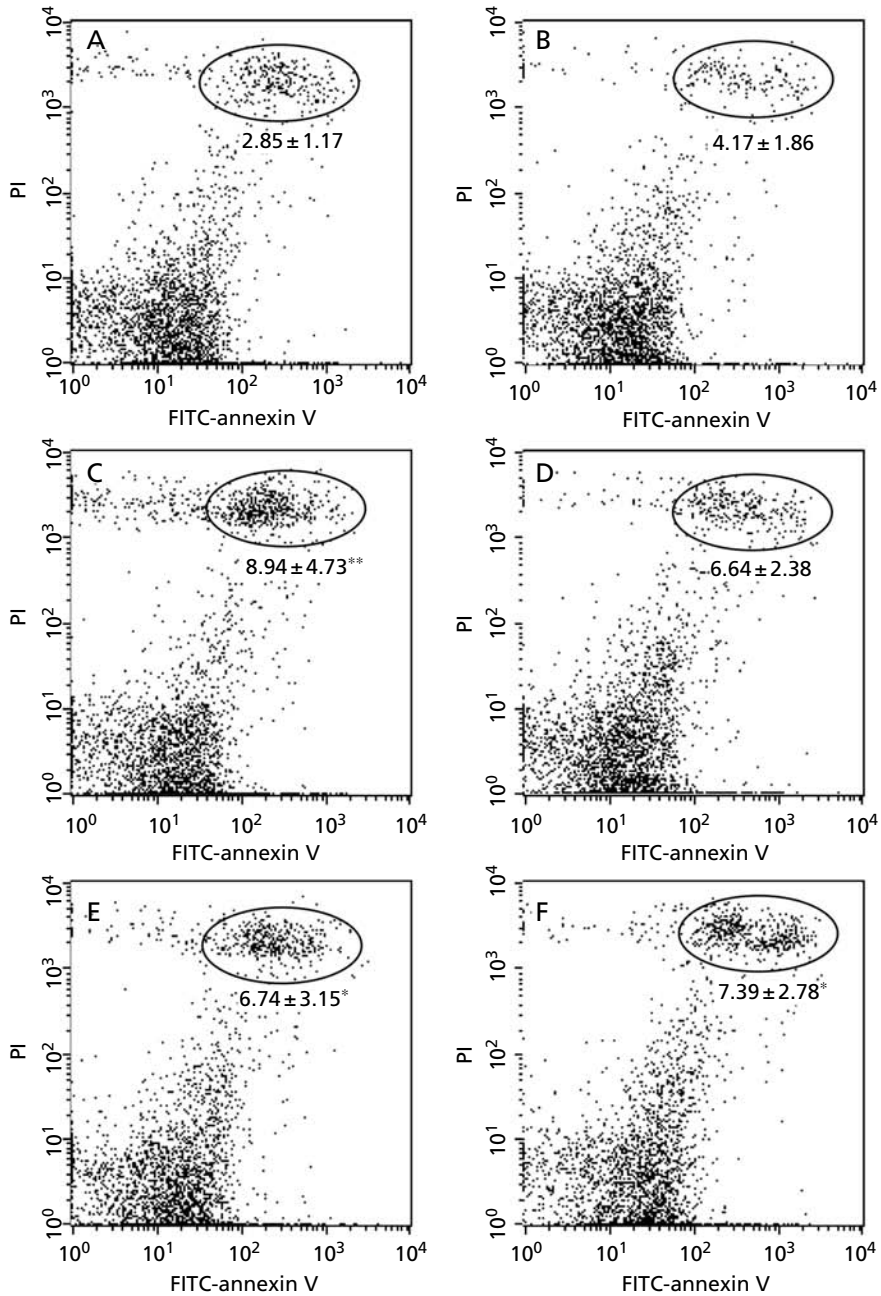

Figure 4 Quantitative analysis of statin-induced apoptosis in L6 using flow cytometry. Myoblasts were treated with statins for 6 h. Each figure shows the typical pattern of FITC-annexin V/propidium iodide (PI) fluorescence. Apoptotic cells were detected in a circle and the percentage represents mean ± s.d. (n = 5). $^{*}P < 0.05$, $^{**}P < 0.01$, compared with control. A, control; B, atorvastatin 3 μM; C, cerivastatin 3 μM; D, fluvastatin 3 μM; E, pravastatin 3 mM; and F, simvastatin 3 μM.

Yonehara (2000) described that activated K-Ras directly inhibited Fas-mediated apoptosis in Fas-transgenic Balb3T3 cells. Since Fas-mediated signal transduction finally executes caspase-8 dependent apoptotic streams, it is much-anticipated that caspase-8 and caspase-3 are activated in statin-treated myoblasts (this hypothesis was summarized in Figure 7B). Supporting this idea, our results showed that statin treatment apparently elevated caspase-8 activity (Figure 6). Taken together, we considered that 'active Ras' depletion from cell membrane directly executed caspase activation and, consequently, skeletal myoblasts caused apoptosis and subsequent severe rhabdomyolysis.

The results showed that cerivastatin directly activated membrane Ras protein (Figure 5B). Contrary to our prediction, this activated Ras was only found in

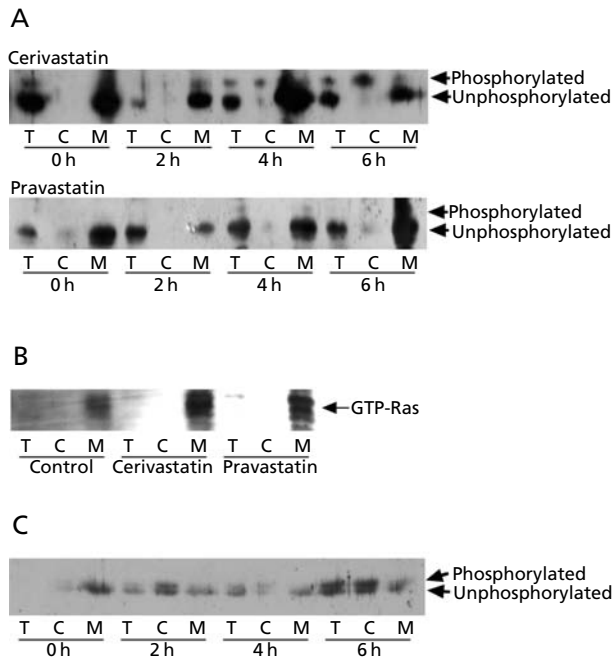

Figure 5 Evaluation of membrane and cytosolic Ras activation. A. Cells were incubated with cerivastatin (3 μM) or pravastatin (3 mM) for 2, 4 or 6 h and membrane or cytosolic fraction underwent electrophoresis onto 12.5% T gel. Arrows represent phosphorylated Ras. B. GTP-bound Ras was concentrated using Raf-1 RBD agarose and applied with SDS-PAGE. T, total cell lysate; C, cytosol; M, membrane. C. Effect of cerivastatin on membrane Rho isoprenylation in L6. Cells were incubated with cerivastatin (3 μM) and assessed for immunoblot analysis.

the membrane fraction, nothing was found in cytosol (despite altered migration distance in SDS-PAGE). Currently, we are unable to explain the phenomenon, however it was clear that cerivastatin itself directly activated membrane Ras protein and consequently Ras drop off from the membrane. Further investigations are needed to clarify the mechanism.

Early apoptosis was determined by fluorescein-staining of FITC-annexin V. On microscopic observation (Figures 1 and 2), there were many green/red fluorescent myoblasts after cerivastatin treatment, more than any other drug. Nevertheless, flow cytometry could only detect a slight increase of apoptotic cells due to cerivastatin. This paradox was attributed to severe induction of apoptosis by cerivastatin itself. Since the onset of apoptosis was severe in cerivastatin-treated myoblasts, the apoptotic body was formed precipitously, and their mass was reduced. Although particles must suspend into sheath fluid for the flow cytometric study, cellular mass reduction might alter the forward and side scatter level, resulting in the lack of apoptosis detection. Further sorting study should improve the exact determination of the apoptotic body.

Conclusion

Our study revealed the mechanism of statin-induced muscular adverse effects, which specifically occurred in skeletal tissue in-vivo. It was determined that the basis of this rhabdomyolysis was the signal transduction of Ras and Rho G proteins. We suggest that flow cytometry could be useful for the exact evaluation of the risk of clinical myopathy.

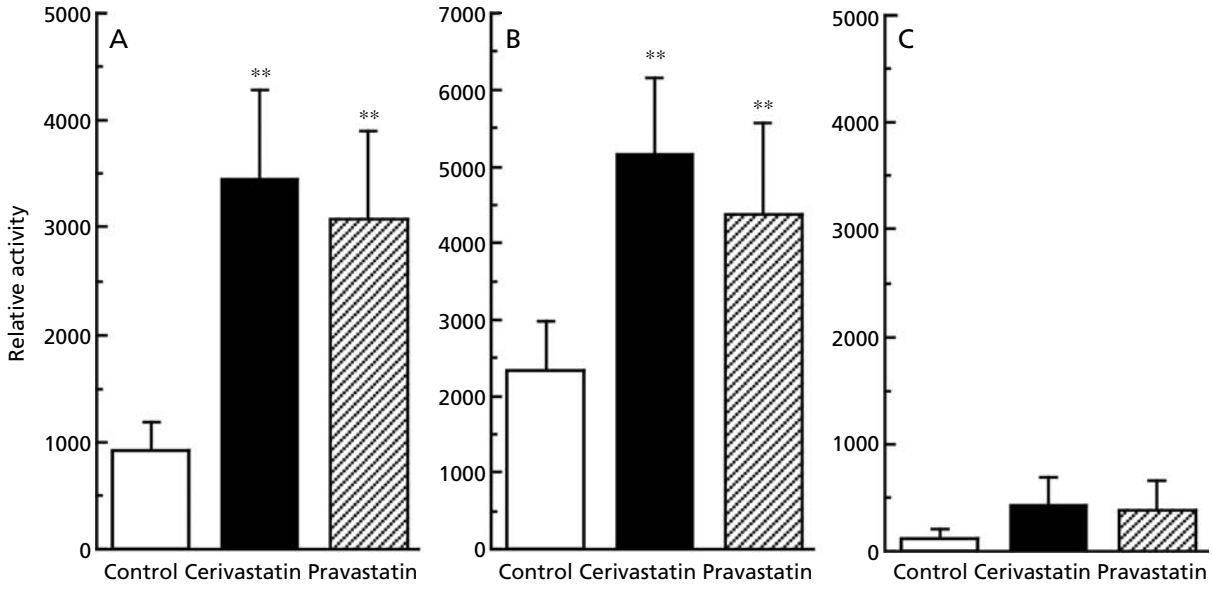

Figure 6 Intracellular caspases activity in statin-treated L6 myoblasts. Cells were cultured for 24 h with cerivastatin (3 μM) or pravastatin (3 mM) and then harvested. Activity of caspase-3 (A), -8 (B) and -9 (C) was determined using their specific substrates. All values represent mean ± s.d. (n = 5–6). $^{**}P < 0.01$, compared with control.

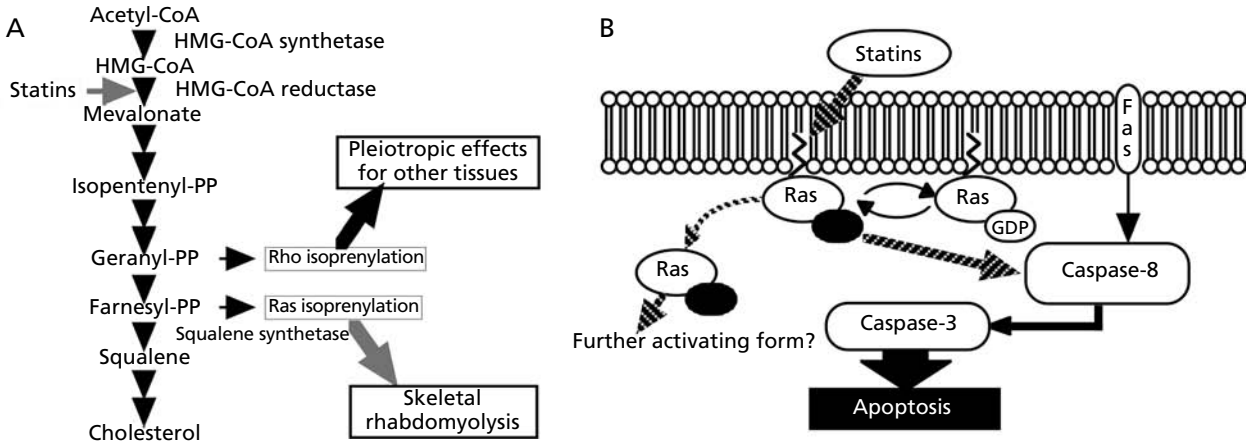

Figure 7 Cholesterol and isoprenoid synthesis pathway (A) and possible mechanism of statin-induced apoptosis (B).

References

Blanco-Colio, L. M., Villa, A., Ortego, M., Hernandez-Presca, M. A., Pascual, A., Plaza, J. J., Egido, J. (2002) 3-Hydroxy-3-methyl-glutaryl coenzyme A reductase inhibitors, atorvastatin and simvastatin, induce apoptosis of vascular smooth muscle cells by downregulation of Bcl-2 expression and Rho A prenylation. *Atherosclerosis* **161**: 17–26

Blanco-Colio, L. M., Munoz-Garcia, B., Martin-Ventura, J. L., Lorz, C., Diaz, C., Hernandez, G., Egido, J. (2003) 3-hydroxy-3-methylglutaryl coenzyme A reductase inhibitors decrease Fas ligand expression and cytotoxicity in activated human T lymphocytes. *Circulation* **108:** 1506–1513

Danesh, F. R., Sadeghi, M. M., Amro, N., Philips, C., Zeng, L., Lin, S., Sahai, A., Kanwar, Y. S. (2002) 3-Hydroxy-3-methyl-glutaryl CoA reductase inhibitors prevent high glucose-induced proliferation of mesangial cells via modulation of Rho GTPase/ p21 signaling pathway: implications for diabetic nephropathy. *Proc. Natl. Acad. Sci. USA* **99**: 8301–8305

Danesh, F. R., Anel, R. L., Zeng, L., Lomasney, J., Sahai, A., Kanwar, Y. S. (2003) Immunomodulatory effects of HMG-CoA reductase inhibitors. *Arch. Immunol. Ther. Exp. (Warsz)* **51**: 139–148

Guijarro, C., Blanco-Colio, L. M., Ortego, M., Alonso, C., Ortiz, A., Plaza, J. J., Diaz, C., Hernandez, G., Egido, J. (1998) 3-Hydroxy-3-methylglutaryl coenzyme a reductase and isoprenylation inhibitors induce apoptosis of vascular smooth muscle cells in culture. *Circ. Res.* **83**: 490–500

Hendriks, F., Kooman, J. P., van der Sande, F. M. (2001) Massive rhabdomyolysis and life threatening hyperkalaemia in a patient with the combination of cerivastatin and gemfibrozil. *Nephrol. Dial. Transplant.* **16**: 2418–2419

Hess, D. C., Demchuk, A. M., Brass, L. M., Yatsu, F. M. (2000) HMG-CoA reductase inhibitors (statins): a promising approach to stroke prevention. *Neurology* **54**: 790–796

Kazama, H., Yonehara, S. (2000) Oncogenic K-Ras and basic fibroblast growth factor prevent Fas-mediated apoptosis in fibroblasts through activation of mitogen-activated protein kinase. *J. Cell Biol.* **148**: 557–566

Kitta, K., Clement, S. A., Remeika, J., Blumberg, J. B., Suzuki, Y. J. (2001) Endothelin-1 induces phosphorylation of GATA-4 transcription factor in the HL-1 atrial-muscle cell line. *Biochem. J.* **359**: 375–380

Laufs, U., Adam, O., Strehlow, K., Wassmann, S., Konkol, C., Laufs, K., Schmidt, W., Bohm, M., Nickenig, G. (2002) Down-regulation of Rac-1 GTPase by estrogen. *J. Biol. Chem.* **278**: 5956–5962

Marsa-Carretero, M., Alos-Manrique, C., Valles-Callol, J. A. (2002) Rhabdomyolysis associated with cerivastatin plus gemfibrozil combined regimen. *Br. J. Gen. Pract.* **52**: 235–236

Matsuyama, K., Nakagawa, K., Nakai, A., Konishi, Y., Nishikata, M., Tanaka, H., Uchida, T. (2002) Evaluation of myopathy risk for HMG-CoA reductase inhibitors by urethane infusion method. *Biol. Pharm. Bull.* **25**: 346–350

Matzno, S., Yamauchi, T., Gohda, M., Ishida, N., Katsuura, K., Hanasaki, Y., Tokunaga, T., Itoh, H., Nakamura, N. (1997) Inhibition of cholesterol biosynthesis by squalene epoxidase inhibitor avoids apoptotic cell death in L6 myoblasts. *J. Lipid Res.* **38**: 1639–1648

Matzno, S., Tazuya, M. K., Tanaka, H., Yasuda, S., Mishima, M., Uchida, T., Nakabayashi, T., Matsuyama, K. (2003) Evaluation of the synergistic adverse effects of concomitant therapy with statins and fibrates on rhabdomyolysis. *J. Pharm. Pharmacol.* **55**: 795–802

Morishima, N., Nakanishi, K., Takenouchi, H., Shibata, T., Yasuhiko, Y. (2002) An endoplasmic reticulum stress-specific caspase cascade in apoptosis. Cytochrome c-independent activation of caspase-9 by caspase-12. *J. Biol. Chem.* **277**: 34287–34294

Ohnaka, K., Shimoda, S., Nawata, H., Shimokawa, H., Kaibuchi, K., Iwamoto, Y., Takayanagi, R. (2001) Pitavastatin enhanced BMP-2 and osteocalcin expression by inhibition of Rho-associated kinase in human osteoblasts. *Biochem. Biophys. Res. Commun.* **287**: 337–342

Ravagnan, L., Roumier, T., Kroemer, G. (2002) Mitochondria, the killer organelles and their weapons. *J. Cell Physiol.* **192**: 131–137

Rodwell, V. W., Nordstrom, J. L., Mitschelen, J. J. (1976) Regulation of HMG-CoA reductase. *Adv. Lipid Res.* **14**: 1–74

Rubins, H. B. (2000) Triglycerides and coronary heart disease: implications of recent clinical trials. *J. Cardiovasc. Risk.* **7**: 339–345

Shek, A., Ferrill, M. J. (2001) Statin–fibrate combination therapy. *Ann. Pharmacother.* **35**: 908–917

Smith, P. F., Eydelloth, R. S., Grossman, S. J., Stubbs, R. J., Schwartz, M. S., Germershausen, J. I., Vyas, K. P., Kari, P. H., MacDonald, J. S. (1991) HMG-CoA reductase

inhibitor-induced myopathy in the rat: cyclosporine A interaction and mechanism studies. *J. Pharmacol. Exp. Ther.* **257**: 1225–1235

Takemoto, M., Liao, J. K. (2001) Pleiotropic effects of 3-hydroxy-3-methylglutaryl coenzyme a reductase inhibitors. *Arterioscler. Thromb. Vasc. Biol.* **21**: 1712–1719

Thornberry, N. A., Rano, T. A., Peterson, E. P., Rasper, D. M., Timkey, T., Garcia, C. M., Houtzager, V. M., Nordstrom, P. A., Roy, S., Vaillancourt, J. P., Chapman, K. T., Nicholson, D. W. (1997) A combinatorial approach defines specificities of members of the caspase family and granzyme B. Functional relationships established for key mediators of apoptosis. *J. Biol. Chem.* **272**: 17907–17911

Towatari, M., May, G. E., Marais, R., Perkins, G. R., Marshall, C. J., Cowley, S., Enver, T. (1995) Regulation of GATA-2 phosphorylation by mitogen-activated protein kinase and interleukin-3. *J. Biol. Chem.* **270**: 4101–4107

Vu, D., Murty, M., McMorran, M. (2001) Statins: rhabdomyolysis and myopathy. *Can. Med. Assoc. J.* **166**: 85–86, 90–91

Zhang, G., Gurtu, V., Kain, S. R., Yan, G. (1997) Early detection of apoptosis using a fluorescent conjugate of annexin V. *Biotechniques* **23**: 525–531

Zimmermann, K. C., Bonzon, C., Green, D. R. (2001) The machinery of programmed cell death. *Pharmacol. Ther.* **92**: 57–70